Supplement: Quantitative imaging of carbon dioxide plumes using a shortwave infrared spectral camera

Marvin Knapp[1], Ralph Kleinschek[1], Sanam N. Vardag[1,3], Felix Külheim[1], Helge Haveresch[1], Moritz Sindram[1], Tim Siegel[1], Bruno Burger[2], and André Butz[1,3,4]

[1]Institute of Environmental Physics (IUP), Heidelberg University, Heidelberg, Germany
[2]Fraunhofer Institute for Solar Energy Systems (ISE), Heidenhofstr. 2, 79110 Freiburg, Germany
[3]Heidelberg Center for the Environment (HCE), Heidelberg University, Heidelberg, Germany
[4]Interdisciplinary Center for Scientific Computing (IWR), Heidelberg University, Heidelberg, Germany

Correspondence: Marvin Knapp (marvin.knapp@uni-heidelberg.de)

Table S1. The table lists the GKM yearly electricity production [TWh] from their annual reports and reported carbon dioxide emissions [Mt] from the E-PRTR. The power plant emits 955 gCO_2/kWh on average.

| Year	Electric Power	CO_2 Emissions
2015	7.779	7.32
2016	8.633	7.88
2017	7.363	6.86
2018	7.185	6.74
2019	4.974	4.92
2020	4.158	4.18
2021	5.167	5.00
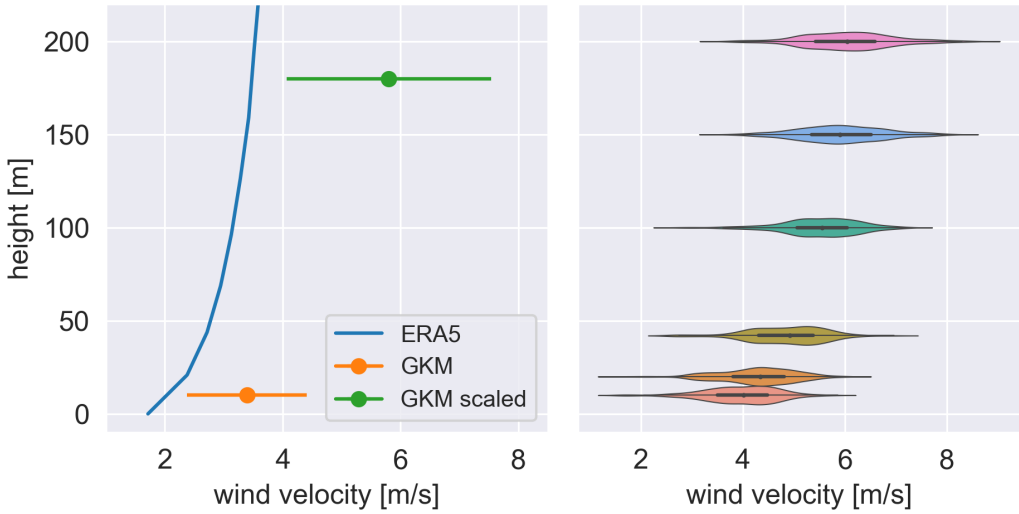
Figure S1. The left panel shows wind data from GKM measured at $10\,\mathrm{m}$ height on September 8th, 2021 (orange). The wind profile is taken from ERA5 and interpolated to the stack location in space and time (blue). The wind velocity is scaled according to the profile to $180\,\mathrm{m}$ (green), the stack tip height of unit 9. The right panel shows the vertically measured wind profile from the Windranger 200 on May 26th, 2022. The distributions are the $2\,\mathrm{min}$ rolling mean values of the absolute wind velocities during the time of observation.

Table S2. Collection of all a priori information. Errors are given as the standard deviation of the quantity during the average time period of the measurement. The subscript a denotes ambient conditions, e denotes the initial plume conditions, and c_0 denotes the CO_2 concentration above the chimney.

Date and time	p_a [hPa]	T_a [°C]	RH [%]	u_a [m/s]	ϕ [°]	T_e [°C]	u_e [m/s]	c_0 [kg/m^3]
2021/09/08 12:13 - 13:15	1016.5 ± 0.1	25.9 ± 0.3	45.5 ± 2.0	7.1 ± 2.2^a	-53 ± 11^a	63.1 ± 0.2	13.4 ± 0.1	0.188 ± 0.002
2021/09/08 13:17 - 14:23	1016.2 ± 0.5	26.8 ± 0.3	40.3 ± 0.9	8.1 ± 1.6^a	-53 ± 11^a	62.9 ± 0.3	13.4 ± 0.1	0.188 ± 0.002
2021/09/08 14:24 - 15:26	1015.3 ± 0.2	27.6 ± 0.2	38.3 ± 0.6	7.6 ± 1.7^a	-51 ± 18^a	63.1 ± 0.1	13.4 ± 0.1	0.188 ± 0.002
2021/09/08 15:27 - 16:35	1014.4 ± 0.2	27.9 ± 0.1	38.1 ± 0.5	7.8 ± 2.1^a	-53 ± 12^a	63.0 ± 0.2	13.3 ± 0.1	0.192 ± 0.002
2022/03/23 14:51 - 16:13	1029.4 ± 0.3	20.0 ± 0.2	25.5 ± 0.1	5.1 ± 0.9^b	33 ± 30^b	60.6 ± 0.1	12.5 ± 0.1	0.201 ± 0.002
2022/03/23 16:14 - 17:36	1028.7 ± 0.1	19.7 ± 0.2	25.1 ± 0.1	3.7 ± 0.9^b	33 ± 25^b	60.6 ± 0.1	12.4 ± 0.1	0.204 ± 0.002
2022/03/26 14:44 - 15:55	1028.2 ± 0.2	20.1 ± 0.1	28.7 ± 0.1	5.6 ± 0.8^b	-97 ± 24^b	61.0 ± 0.3	7.4 ± 0.4	0.131 ± 0.012
2022/03/26 15:56 - 17:36	1027.7 ± 0.0	19.9 ± 0.2	28.7 ± 0.3	6.0 ± 0.7^b	-109 ± 23^b	59.3 ± 0.2	11.1 ± 1.8	0.179 ± 0.055
2022/03/28 15:35 - 16:28	1019.9 ± 0.3	22.6 ± 0.2	33.4 ± 0.2	2.9 ± 0.7^b	-60 ± 34^b	59.0 ± 0.5	11.3 ± 0.5	0.185 ± 0.013
2022/05/13 12:21 - 14:01	1020.2 ± 0.1	25.4 ± 0.3	34.2 ± 1.5	5.4 ± 0.8^b	72 ± 44^b	62.3 ± 0.7	12.1 ± 0.1	0.427 ± 0.053
2022/05/13 14:02 - 15:39	1020.0 ± 0.1	25.3 ± 0.3	32.5 ± 0.4	5.6 ± 0.9^b	80 ± 37^b	61.9 ± 0.3	12.8 ± 1.1	0.259 ± 0.070

[a] from ERA5 scaling of the GKM 10 m wind field.

[b] from Lidar observation
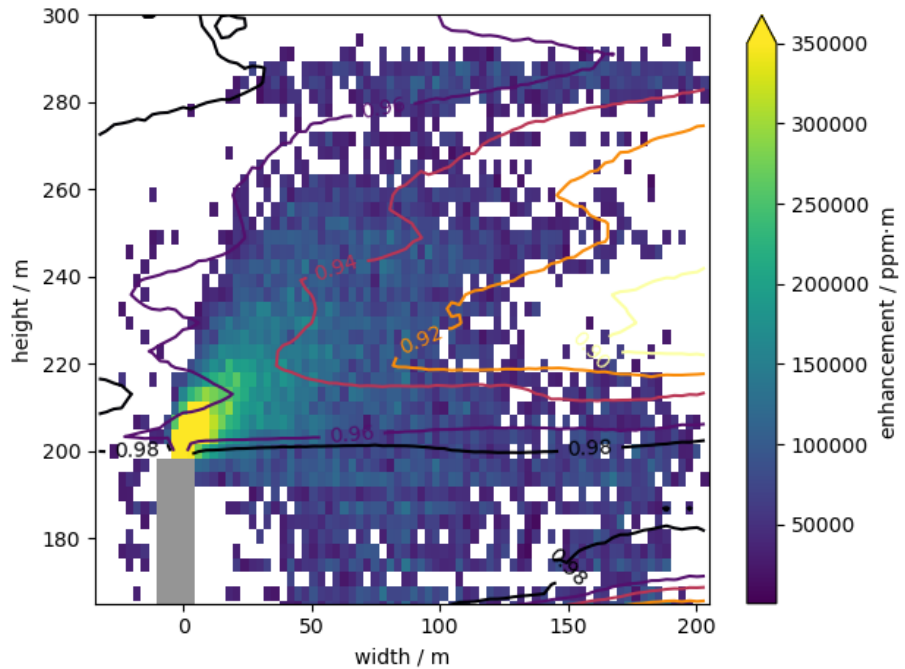
Figure S2. The colored pixels are the retrieved enhancements from 14:02 - 15:39 UTC on 2022/05/13. The gray area marks the chimney of unit 6. Contour lines indicate the background brightness at 2095 nm, a wavelength unaffected by CO_2 absorption. The observed plume widens unexpectedly after emission and a wide stripe of enhancements below the emission height is visible. Furthermore, around 290 m height, another stripe of enhancements is visible. Both features, irrespective of their source, cannot be reproduced by the Gaussian plume model. Thus, we consider these observations unsuited for emission interpretation.
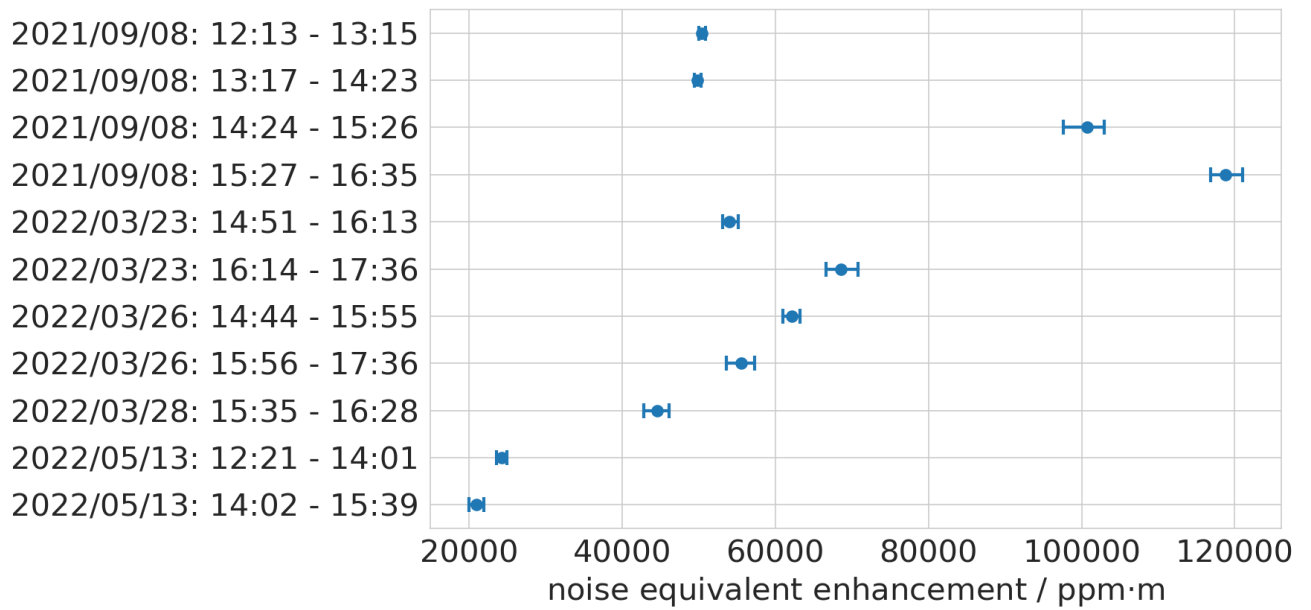
Figure S3. The noise equivalent enhancement σ_j (equation (**??**)) for every observation. The dots mark the plume mean and the error bars minimum and maximum within the plume mask.
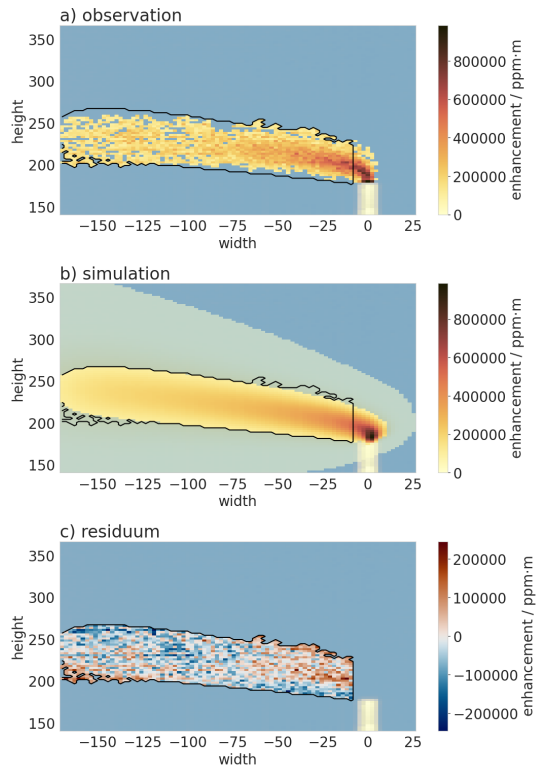
Figure S4. Best fitting plume for 2021/09/08 12:13 - 13:15.
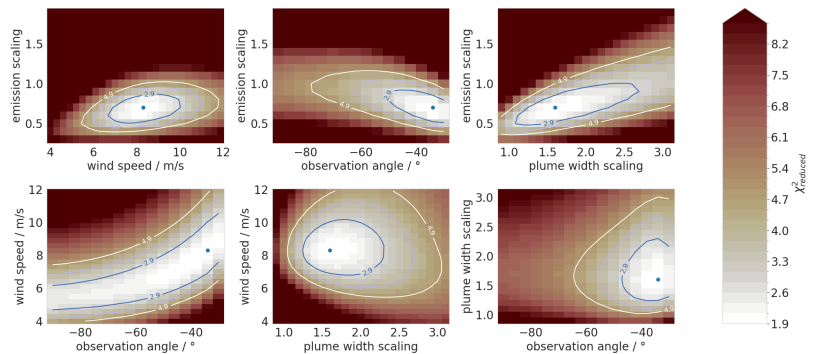
Figure S5. Hypersurfaces of χ_r^2 cost function for 2021/09/08 12:13 - 13:15.
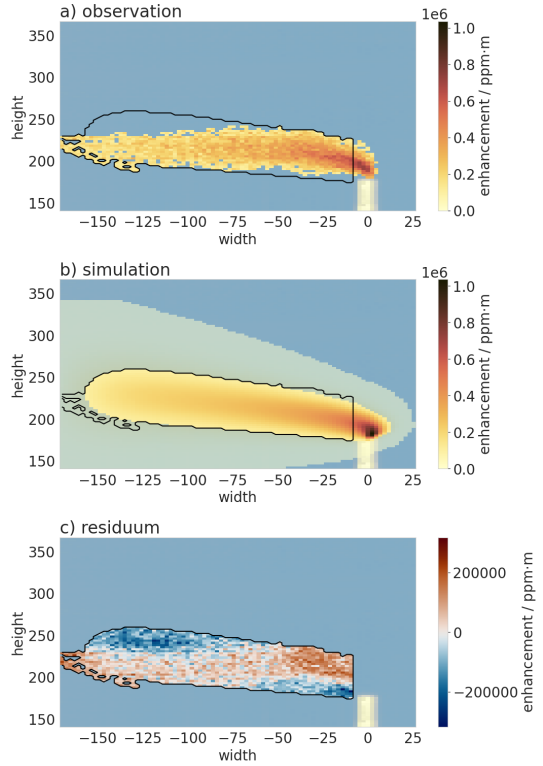
Figure S6. Best fitting plume for 2021/09/08 13:17 - 14:23.
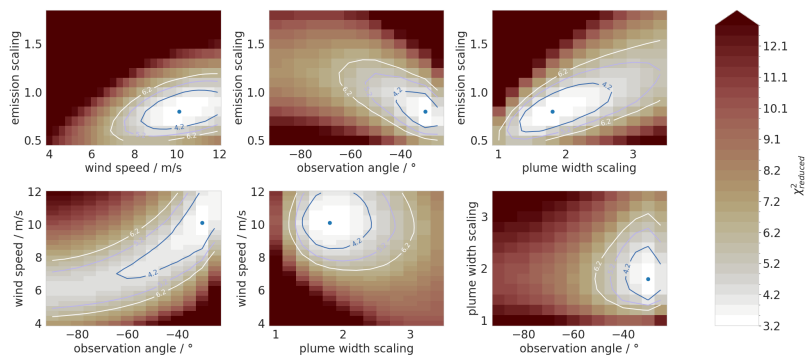
Figure S7. Hypersurfaces of χ_r^2 for 2021/09/08 13:17 - 14:23.
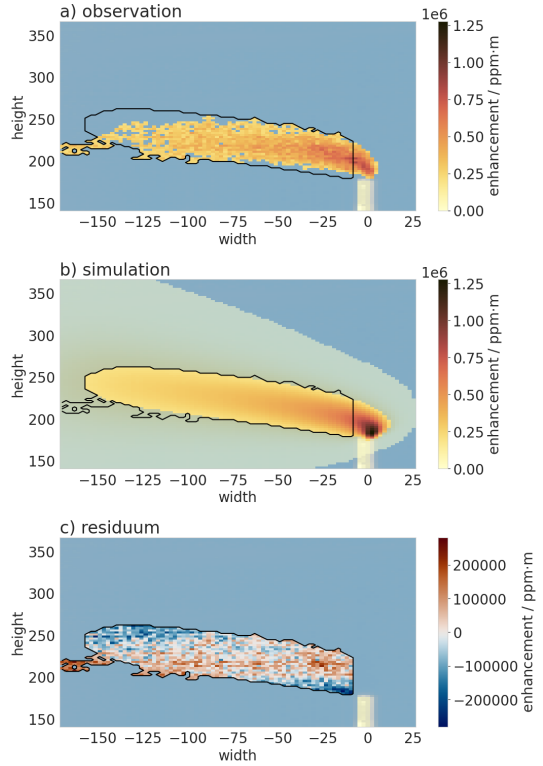
Figure S8. Best fitting plume for 2021/09/08 14:24 - 15:26.
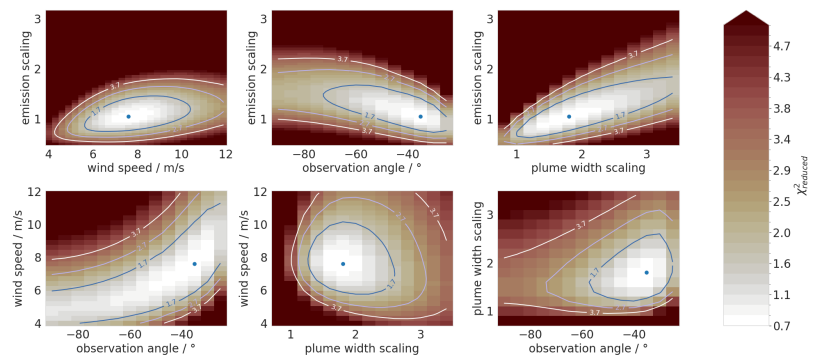
Figure S9. Hypersurfaces of χ_r^2 cost function for 2021/09/08 14:24 - 15:26.
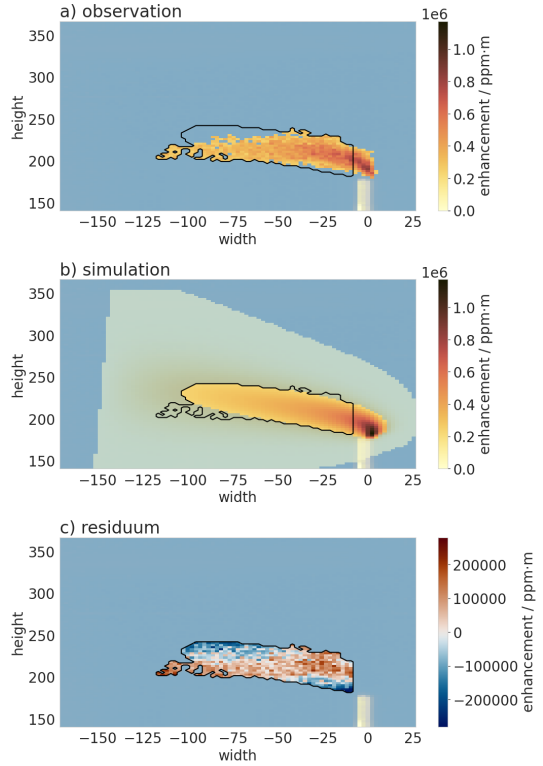
Figure S10. Best fitting plume for 2021/09/08 15:27 - 16:35.
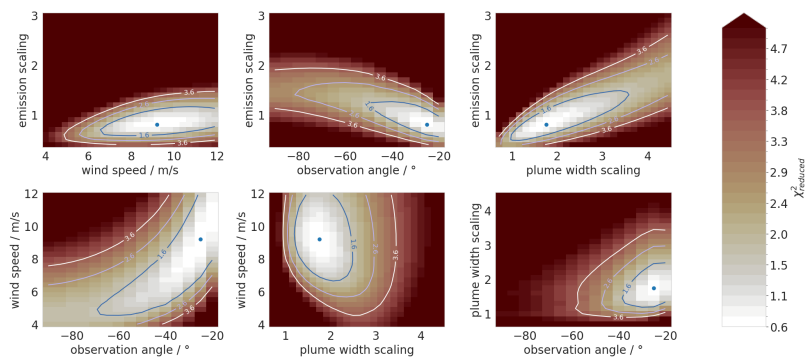
Figure S11. Hypersurfaces of χ_r^2 cost function for 2021/09/08 15:27 - 16:35.
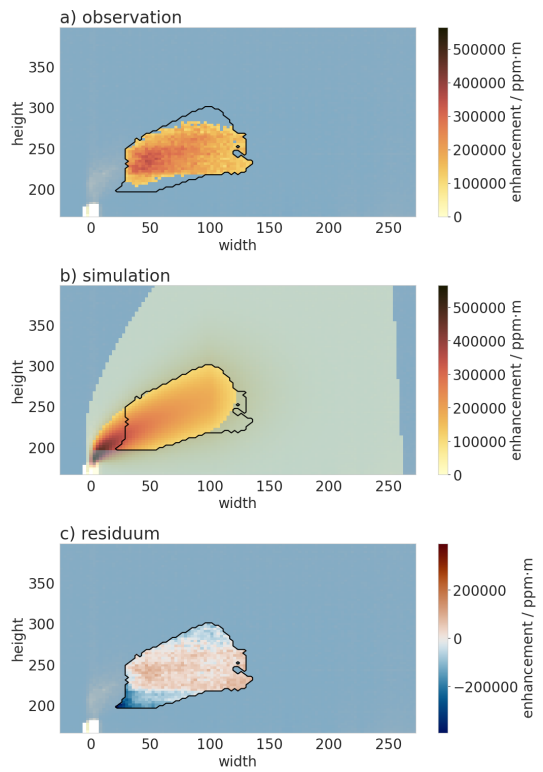
Figure S12. Best fitting plume for 2022/03/23 14:51 - 16:13.
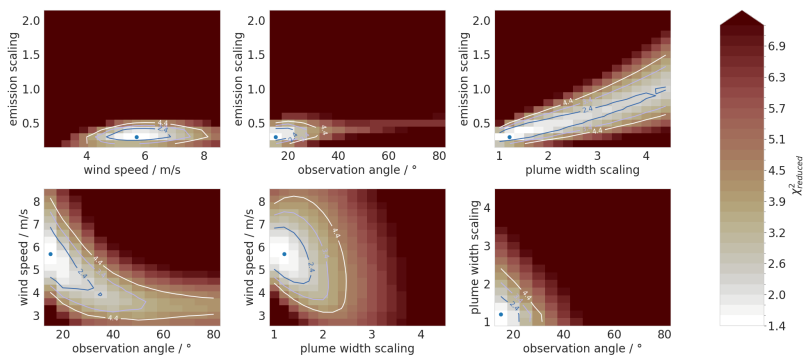
Figure S13. Hypersurfaces of χ_r^2 cost function for 2022/03/23 14:51 - 16:13.
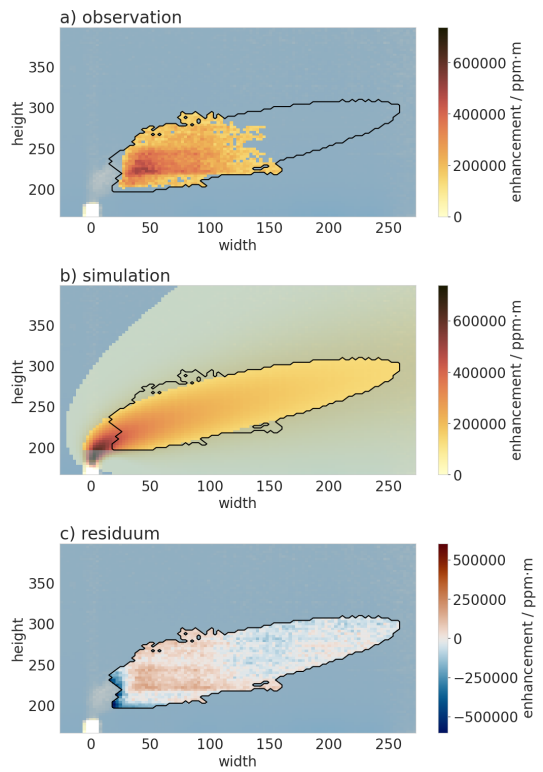
Figure S14. Best fitting plume for 2022/03/23 14:51 - 16:13.
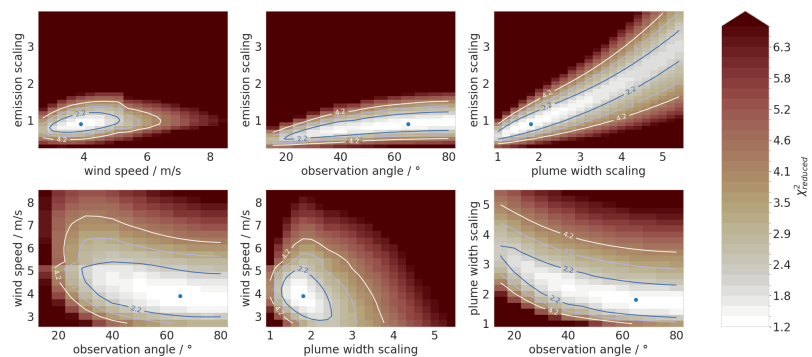
Figure S15. Hypersurfaces of χ_r^2 cost function for 2022/03/23 14:51 - 16:13.
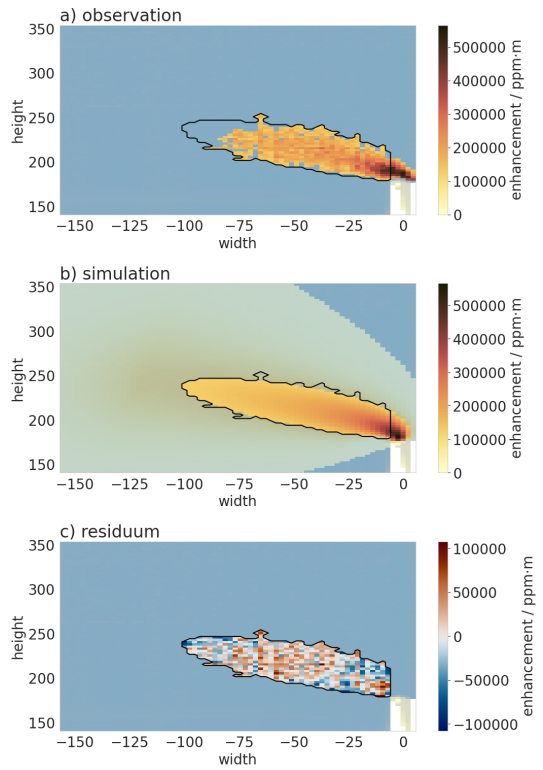
Figure S16. Best fitting plume for 2022/03/26 14:44 - 15:55.
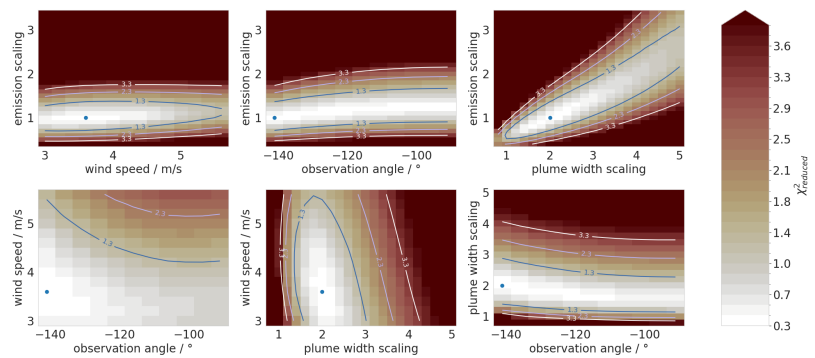
Figure S17. Hypersurfaces of χ_r^2 cost function for 2022/03/26 14:44 - 15:55.
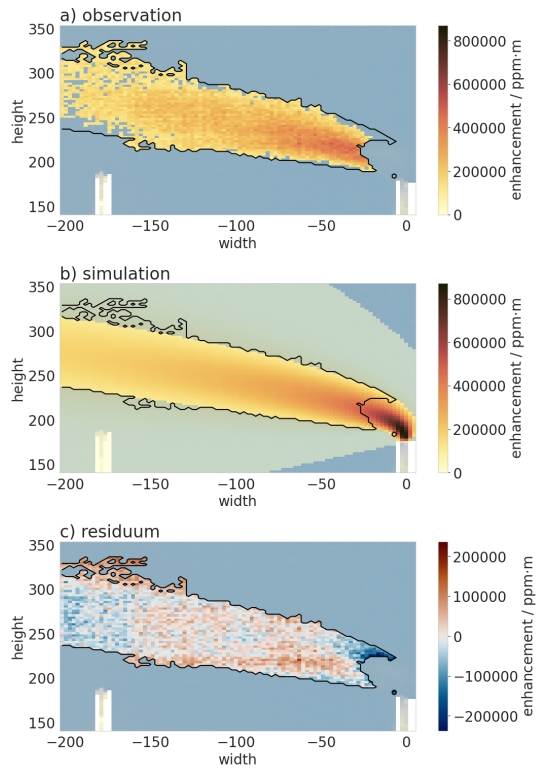
Figure S18. Best fitting plume for 2022/03/26 15:56 - 17:36.
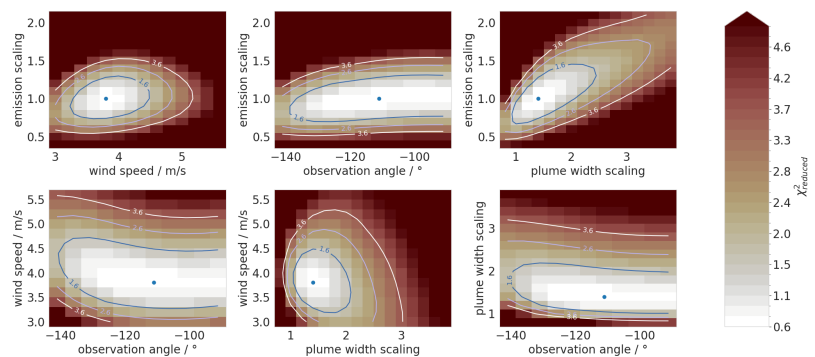
Figure S19. Hypersurfaces of χ_r^2 cost function for 2022/03/26 15:56 - 17:36.
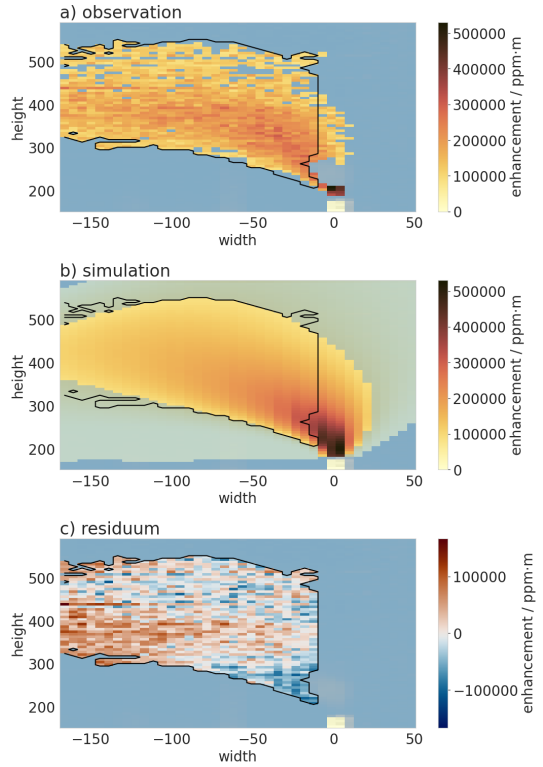
**Figure S20.** Best fitting plume for 2022/03/28 14:41 - 16:28.
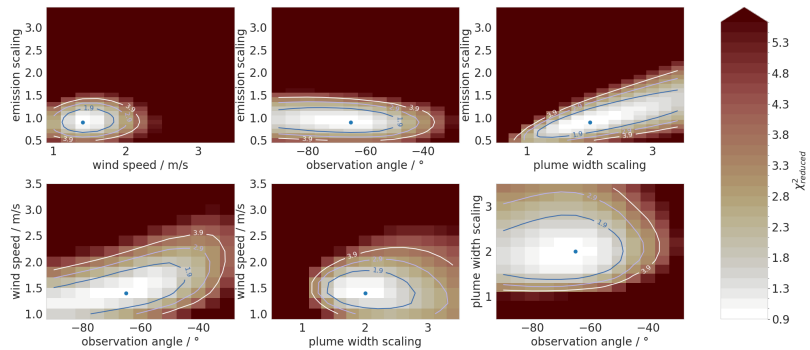
**Figure S21.** Hypersurfaces of χ_r^2 cost function for 2022/03/28 14:41 - 16:28.
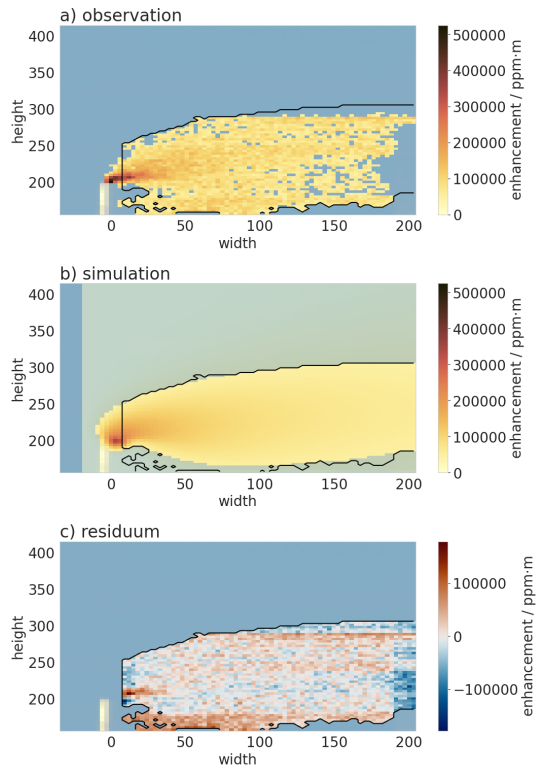
Figure S22. Best fitting plume for 2022/05/13 12:21 - 14:01.
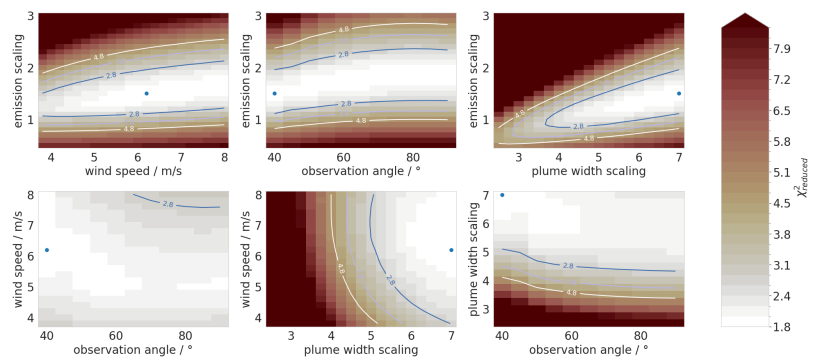

Figure S23. Hypersurfaces of χ_r^2 cost function for 2022/05/13 12:21 - 14:01.
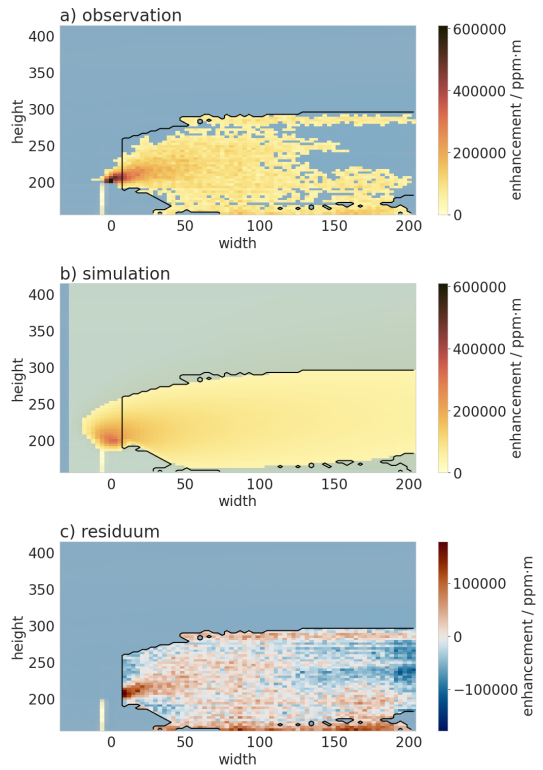
**Figure S24.** Best fitting plume for 2022/05/13 14:02 - 15:39.
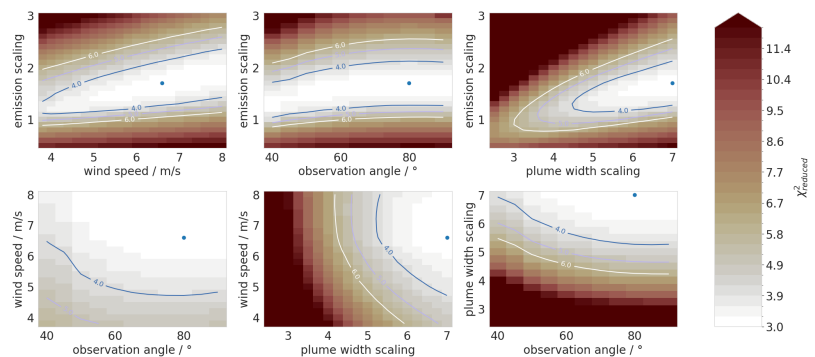
Figure S25. Hypersurfaces of χ_r^2 cost function for 2022/05/13 14:02 - 15:39.